Semi-automated Extraction of Crohns Disease MR Imaging Markers Using a 3D Residual CNN with Distance Prior

Yechiel Lamash(✉), Sila Kurugol, and Simon K. Warfield

Boston Children's Hospital and Harvard Medical School, Boston, USA
shilikster@gmail.com

Abstract. We propose a 3D residual convolutional neural network (CNN) algorithm with an integrated distance prior for segmenting the small bowel lumen and wall to enable extraction of pediatric Crohns disease (pCD) imaging markers from T1-weighted contrast-enhanced MR images. Our proposed segmentation framework enables, for the first time, to quantitatively assess luminal narrowing and dilation in CD aimed at optimizing surgical decisions as well as analyzing bowel wall thickness and tissue enhancement for assessment of response to therapy. Given seed points along the bowel lumen, the proposed algorithm automatically extracts 3D image patches centered on these points and a distance map from the interpolated centerline. These 3D patches and corresponding distance map are jointly used by the proposed residual CNN architecture to segment the lumen and the wall, and to extract imaging markers. Due to lack of available training data, we also propose a novel and efficient semi-automated segmentation algorithm based on graph-cuts technique as well as a software tool for quickly editing labeled data that was used to train our proposed CNN model. The method which is based on curved planar reformation of the small bowel is also useful for visualizing, manually refining, and measuring pCD imaging markers. In preliminary experiments, our CNN network obtained Dice coefficients of $75 \pm 18\%$, $81 \pm 8\%$ and $97 \pm 2\%$ for the lumen, wall and background, respectively.

1 Introduction

Magnetic resonance enterography (MRE) has emerged as a most effective method for imaging the small bowel in patients with Crohns disease (CD) [1]. Extracting CD biomarkers is essential for staging disease, selecting treatment, and assessing therapeutic response. Moreover, our ability to segment diseased bowel will facilitate automated computation of quantitative imaging markers such as length of involvement, wall thickness, lumen narrowing, stricture length, upstream dilation and tissue contrast enhancement. Several methods [2–5] have been proposed for segmenting the small bowel wall. However, all these methods segment the wall and lumen together from their background instead of each compartment alone. In addition, they do not provide the small bowel's tube structure that is

D. Stoyanov et al. (Eds.): DLMIA 2018/ML-CDS 2018, LNCS 11045, pp. 218–226, 2018.
https://doi.org/10.1007/978-3-030-00889-5_25

necessary for computing disease markers such as wall thickness or lumen narrowing. Instead they mark disjoint tissue segments with Crohns disease. Deep learning algorithms, in particular, convolutional neural networks, have rapidly become a methodology of choice for analyzing medical images [6]. Thanks to its unique capability of learning hierarchical feature representations solely from data, deep learning has achieved record-breaking performance in a variety of artificial intelligence applications and grand challenges [7]. Such networks generally have large number of parameters and training them requires a correspondingly large dataset. However, there is not enough publicly available datasets and it is labor intensive to manually label images for segmentation. Moreover, in our problem specifically, there is no training data available at all.

Our first contribution in this work is the development of an efficient software platform for semi-automated segmentation and labeling of pCD accomplished with curved planar reformation (CPR) of small bowel segments. Our proposed software platform generates segmentation of the bowel wall and lumen using a graph-cuts algorithm given a series of seed points located on the lumens centerline. The tool also allows for efficient and quick manual editing of the segmentation results on straightened CPR views as well as visualizing the entire diseased bowel region in a stretched CPR view. We used this semi-automated tool to generate training data for our proposed segmentation algorithm. Our second contribution is a 3D residual CNN network with a distance prior for improved segmentation of the bowel lumen and wall, and extraction of quantitative imaging markers.

2 Method

2.1 Efficient Semi-automated Software for Generating Labeled Training Data for Pediatric Crohn's Disease

To generate a labeled dataset efficiently, we perform the following steps shown in Fig. 1: First, we generate a CPR platform that flattens the small bowel segment. Next, we use a graph cut segmentation [8,9] to obtain an initial segmentation of the bowel wall boundaries. We then manually refine the segmentation contours on straightened CPR images using the proposed tool. Last, we generate a tetrahedral mesh to transfer the segmentations represented by the contours in the straightened CPR views into a volumetric representation. The sections below describe each of these steps.

Generation of CPR Views for the Small Bowel. The first step entails placing seed points along the lumens centerline. We developed a practical and robust platform to perform this task such that seeds can be placed in coronal, sagittal and axial views that are automatically synchronized to the users cursor location. This enables the operator to select seed points in the most visible cross-section along the curved lumen. In the event the lumen is completely obstructed, we select seed points in the middle of the obstruction. We then interpolate between the seed points to obtain a curve $r(t) = [x(t), y(t), z(t)]$. Next,

we perform arclength parameterization [10] to obtain an equally sampled curve. For generating a stretched CPR view, we perform the following steps: (1) select a plane that transverses through the two extreme points of the centerline as well as an additional, interactively selected point; (2) project the curve onto that plane; (3) perform arclength parameterization [10] of the projected curve; and (4) interpolate the stretched CPR image by traversing along the projected curve at equal speed where each step is a ray perpendicular to the projected curve.
For straightened CPR view, we set the Frenet-Serret frame [11] along the curve and interpolate images on the curves normal planes. Before calculating the Frenet-Serret frame vectors, we applied Savitzky-Golay filtering [12] to smooth the centerline curve as well as the orthogonal vectors along it.

Graph Cut Segmentation. A graph cut algorithm is used to segment the bowel lumen and wall in the CPR volume. Due to the axis-symmetric representation of the bowel in the reconstructed straightened CPR volume, we define the connectivity of the graph to be between pixels represented in cylindrical coordinates $[r, z, \theta]$. We therefore sample straightened CPR images every 5 degrees to generate a volume where each image represents a slice that passes through the center at a specific angle θ. Using this representation, we segment the volume into five classes: upper background, upper wall, lumen, lower wall, and lower background. After obtaining the segmentation results, we extract the contours of the wall and the lumen and then manually refine the results using the visual interface. The editing is performed on six discrete angles and with interpolation in between.

Projection of the Labeling onto Coronal Images. We use a method similar to [13]. Given the segmentation boundaries in the CPR view, we construct a tetrahedral mesh. We then assign the voxels of each tetrahedron in the mesh with either lumen or wall label. To do so, we perform the following: Given a tetrahedron T, any point $p \in T$ divides it into four sub tetrahedrons such that the vector e of the point p with respect to vertex v can be expressed by $e = \alpha e_i + \beta e_j + \gamma e_k$, where the barycentric coordinates $(\alpha, \beta, \gamma) \in (0, 1)$ are the volume ratios between each sub-tetrahedron and tetrahedron T.

$$\alpha = \frac{\det(e, e_j, e_k)}{\det(e_i, e_j, e_k)}; \beta = \frac{\det(e_i, e, e_k)}{\det(e_i, e_j, e_k)}; \gamma = \frac{\det(e_i, e_j, e)}{\det(e_i, e_j, e_k)} \tag{1}$$

e_i, e_j, e_k are the tetrahedron edge vectors with respect to vertex v.
To find the inner voxels surrounded by each tetrahedron, we take the grid pixels of the minimal box that bounds the tetrahedron and looked up the pixels whose barycentric coordinates apply: $\alpha, \beta, \gamma \geq 0$ and $\alpha + \beta + \gamma \leq 1$.

2.2 Segmentation of the Bowel Lumen and Wall Using a 3D Residual CNN with Distance Prior

Our motivation for using a 3D CNN segmentation algorithm is based on the observation that the highly variable bowel appearance and shape requires a

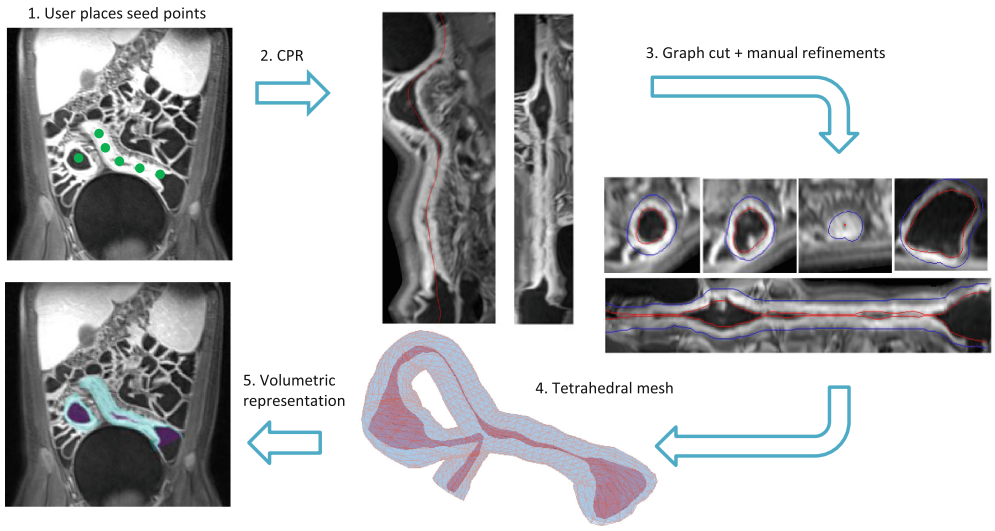

Fig. 1. Generation of labeled dataset of Crohns disease segments.

supervised algorithm that can learn feature representations and a classifier from a large set of augmented training patches for solving this difficult problem. We perform the segmentation in the original coronal image volumes instead of using CPR views to eliminate the dependency of the performance on the initial centerline delineation. The segmentation of the small bowel is challenging because one diseased section of the wall can be adjacent to either part of the same diseased segment, or part of a distal healthy segment. In addition, the lumen and the mesentery might have similar intensities such that from a patch perspective, it may be unclear whether a region is inside the lumen or between two walls. To overcome this ambiguity, we added a distance map prior to the input data. Accordingly, the distance prior is computed as the shortest distance of each voxel from the interpolated centerline seed points-positioned in the lumen.

Our CNN network, shown in Fig. 2, has a 3D fully connected U-Net architecture [14] with residual units [15]. The network has three contracting layers; three expanding layers; and a final convolution layer (with kernel size one) followed by softmax. Each residual layer has two sets of batch normalization (BN), leaky ReLU activation, and convolution as suggested by [15]. Down-sampling and up-sampling of features is done using strided convolutions and transpose convolutions, respectively. The input to the network consists of two channel patches $64 \times 64 \times 32$ in size. The first channel patches were taken from the contrast-enhanced T1-weighted MR images after resampling to isotropic resolution. Before cropping the patches, the images are normalized to have zero mean and a standard deviation equal to 1. In the training, the patches were centered on randomly selected lumen or wall pixels. We scale the distances to the range of $[-1, 1]$ after truncating the max value to 32. We trained the network with a stochastic gradient descent with momentum of 0.9 and L_2 regularization with $\lambda = 10^{-3}$. To augment the training data, we added Gaussian noise, random rotations over the x-axis, random scaling of $\pm 10\%$, and random flips in each of

the three dimensions. The augmentation generated >2 million patches - each contains a short tube segment of the small bowel in an arbitrary shape and orientation.

3 Experiments and Results

We used contrast-enhanced T1-weighted MR images of 23 pediatric patients with Crohns disease. The images were scanned in coronal planes with voxel size of about $0.75 \times 0.75 \times 2\,\text{mm}$. We interpolated the image to isotropic sampling of 0.75 m before the analysis. We generated a labeled dataset of the small bowel lumen and wall as described above. We divided the dataset into a training set of 15 patients and a test set of 8 patients from which we extract 3D patches for training and testing the proposed segmentation network, respectively. To evaluate the accuracy of the segmentation, we computed the Dice Similarity Coefficient (DSC) of the lumen wall and background classes. In addition, we computed the distances between the CNN boundary contours and the label boundary contours.

Figure 3 demonstrates the results of the proposed lumen and wall segmentation algorithm on 4 patients compared to the ground truth labels in the original coronal plane and after reformation of the segmentation results into the straightened CPR views. Table 1 summarizes the performance of our model in segmenting the small bowel lumen and wall. When integrating the proposed distance prior into the proposed 3D Residual U-Nets architecture, the Dice coefficients increased from 55% to 75% for the lumen and from 60% to 81% for the wall segment. The median distance between the automated and manually labeled contours reduced from 1.70 mm to 0.85 mm and from 1.6 mm to 1.0 mm for the lumen-wall and wall-background boundaries, respectively.

Figure 4 shows surface rendering of diseased bowel loops and their corresponding imaging markers from 4 patients. The upper row shows the lumen radius and the lower row shows the thickness of the bowel wall. Figure 4 cases (a) and (d) shows diseased areas with strictures that have a very narrow lumen

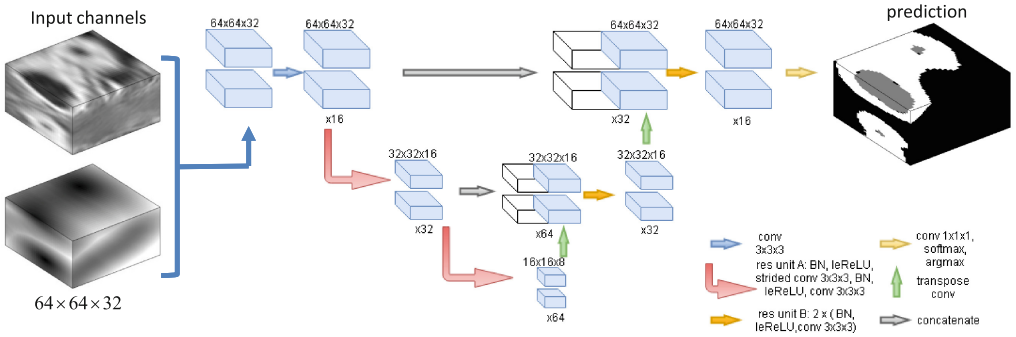

Fig. 2. The networks input patches and its architecture. (To better demonstrate, the two input channels are depicted one above the other, and the residual U-Nets concatenating channels are depicted alongside one another.)

and thickened bowel wall. These markers are useful for surgical planning (a, d) and for quantitatively evaluating disease severity (b, c).

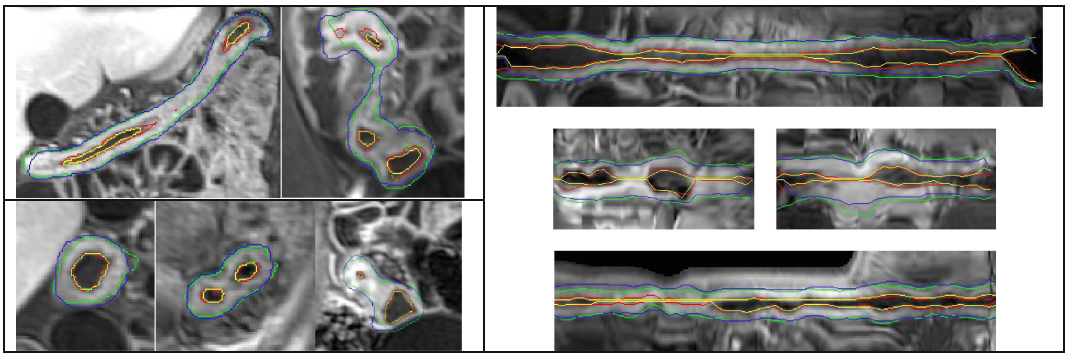

Fig. 3. The results of the proposed segmentation algorithm of the lumen and wall of 4 patients compared to the labels in coronal planes (left) and in straightened CPR views (Right). Color coding: lumen-wall contours CNN (yellow) vs. label (red). Wall-background contours CNN (blue) vs. label (green). (Color figure online)

Table 1. Performance of the network in segmenting the small bowel lumen and wall. DSC-Dice Similarity Coefficient, BD- Boundaries Distance (between the CNN result and the label).

	DSC [%] lumen	DSC [%] wall	DSC [%] back-ground	Cross entropy	Median BD [mm] lumen	Median BD [mm] wall	Average BD [mm] lumen	Average BD [mm] wall
Single input channel	55 ± 25	60 ± 17	93 ± 4	0.33	0.83 ± 2.8	1.7 ± 4.0	1.6 ± 2.8	3.4 ± 4.0
Distance prior concatenated at the final layer	70 ± 19	75 ± 10	95 ± 4	0.22	0.83 ± 1.8	1.8 ± 3.1	1.2 ± 1.8	3.1 ± 3.1
Distance channel prior (proposed)	75 ± 18	81 ± 8	97 ± 2	0.13	0.83 ± 1.5	0.85 ± 2.3	1.0 ± 1.5	1.8 ± 2.3

Table 2. Comparison to Crohns disease small bowel segmentation prior work.

Method	Provide the entire disease segment?	Provide disease mark-ers?	DSC [%] lumen	DSC [%] wall	DSC [%] back-ground	DSC [%] lumen+wall vs. background
SL [2]	No	No	N/A	N/A	N/A	86.5 ± 2.3
SS-AL [4]	No	No	N/A	N/A	N/A	92.1
AS [3]	No	No	N/A	N/A	N/A	90 ± 4
AL [5]	No	No	N/A	N/A	N/A	92.7
CNN (ours)	Yes	Yes	75 ± 18	81 ± 8	97 ± 2	N/A

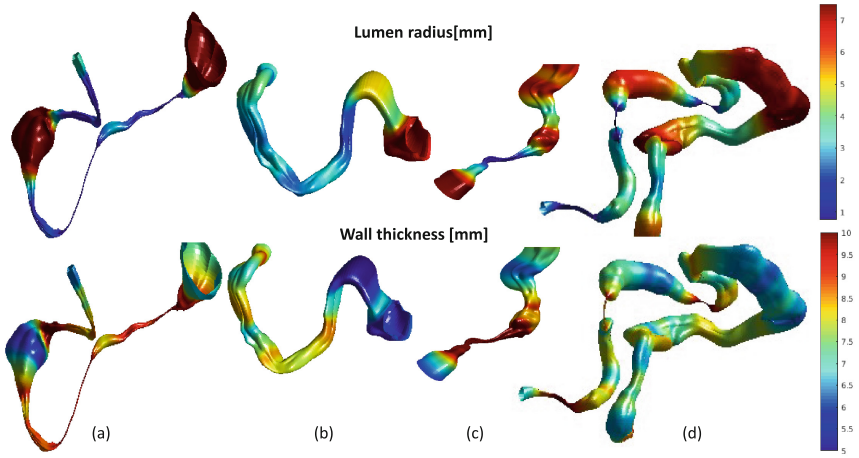

Fig. 4. Surface rendering of the lumen boundary with colormaps indicating lumen radius [mm] (upper row) and wall thickness [mm] (lower row) obtained using the proposed method. Cases (a) and (d) has diseased areas with strictures that have a very narrow lumen and a very thickened bowel wall that may indicate surgical therapy.

4 Discussion and Conclusions

We propose a novel algorithm for segmenting both the bowel lumen and wall in T1-weighted, contrast-enhanced MR images and extracting imaging markers of pediatric Crohns disease including bowel wall thickness and lumen radius. Our algorithm is based on a 3D residual CNN with a distance prior that improved the performance compared to a 3D residual CNN without the distance prior. The performance when adding the distance map as an additional channel was superior to that seen when integrating the distance prior at the final layer -an observation that implies that integrating spatial information to the learned filters will improve overall performance. Such spatial informative channels may improve the performance in other image segmentation applications as well. We observed that, there were several locations where the algorithm delineated the boundaries more accurately than the labeled data. For cases that require manual refinement, our proposed editing software enables efficient and quick manual editing of the segmentations on CPR views before computing the disease markers. All prior works with reported segmentation performance segment the wall and lumen together from their background instead of each compartment alone. These works provide small tissue segments with Crohns disease instead of tube structure and therefore cannot extract the wall thickness or lumen narrowing (Table 2). The limitation of our method, however, is the difficulty in placement of seed points along the centerline in images with high motion artifacts, insufficient bowel preparation or

severe disease condition where the lumen path is barely visible. We anticipate the proposed method and the automatically extracted imaging markers will facilitate comprehensive assessment of diseased bowel lumen and wall in pediatric Crohns disease.[1]

References

1. Bruining, D.H., Zimmermann, E.M., Loftus, E.V., Sandborn, W.J., Sauer, C.G., Strong, S.A.: Consensus recommendations for evaluation, interpretation, and utilization of computed tomography and magnetic resonance enterography in patients with small bowel Crohns disease. Gastroenterology **154**(4), 1172–1194 (2018)
2. Mahapatra, D., Schueffler, P., Tielbeek, J.A.W., Buhmann, J.M., Vos, F.M.: A supervised learning based approach to detect Crohn's disease in abdominal MR volumes. In: Yoshida, H., Hawkes, D., Vannier, M.W. (eds.) ABD-MICCAI 2012. LNCS, vol. 7601, pp. 97–106. Springer, Heidelberg (2012). https://doi.org/10.1007/978-3-642-33612-6_11
3. Mahapatra, D.: Automatic detection and segmentation of Crohn's disease tissues from abdominal MRI. IEEE Trans. Med. Imaging **32**(12), 2332–2347 (2013)
4. Mahapatra, D., Schüffler, P.J., Tielbeek, J.A.W., Vos, F.M., Buhmann, J.M.: Semi-supervised and active learning for automatic segmentation of Crohn's disease. In: Mori, K., Sakuma, I., Sato, Y., Barillot, C., Navab, N. (eds.) MICCAI 2013. LNCS, vol. 8150, pp. 214–221. Springer, Heidelberg (2013). https://doi.org/10.1007/978-3-642-40763-5_27
5. Mahapatra, D., et al.: Active learning based segmentation of Crohn's disease using principles of visual saliency. In: 2014 IEEE 11th International Symposium on Biomedical Imaging (ISBI), pp. 226–229. IEEE (2014)
6. Litjens, G.: A survey on deep learning in medical image analysis. Med. Image Anal. **42**, 60–88 (2017)
7. Shen, D., Guorong, W., Suk, H.-I.: Deep learning in medical image analysis. Annu. Rev. Biomed. Eng. **19**, 221–248 (2017)
8. Boykov, Y., Funka-Lea, G.: Graph cuts and efficient ND image segmentation. Int. J. Comput. Vis. **70**(2), 109–131 (2006)
9. Bagon, S.: Matlab wrapper for graph cut, December 2006. http://www.wisdom.weizmann.ac.il/~bagon
10. Willmore, T.J.: An Introduction to Differential Geometry. Courier Corporation (2013)
11. Weatherburn, C.E.: Differential Geometry of Three Dimensions, vol. 1. Cambridge University Press, Cambridge (2016)
12. Orfanidis, S.J.: Introduction to signal processing. **7458**, 168–383 (1996). Prentice-Hall, Inc. Upper Saddle River
13. Lamash, Y., Fischer, A., Carasso, S., Lessick, J.: Strain analysis from 4-D cardiac CT image data. IEEE Trans. Biomed. Eng. **62**(2), 511–521 (2015)

[1] This work is supported by Crohns and Colitis Foundation of Americas Career Development Award, AGA-Boston Scientific Technology & Innovation Pilot Research Award, and the National Institute of Diabetes and Digestive and Kidney Diseases (NIDDK) of the NIH under award R01DK100404.

14. Ronneberger, O., Fischer, P., Brox, T.: U-Net: convolutional networks for biomedical image segmentation. In: Navab, N., Hornegger, J., Wells, W.M., Frangi, A.F. (eds.) MICCAI 2015. LNCS, vol. 9351, pp. 234–241. Springer, Cham (2015). https://doi.org/10.1007/978-3-319-24574-4_28
15. He, K., Zhang, X., Ren, S., Sun, J.: Deep residual learning for image recognition. In: Proceedings of the IEEE Conference on Computer Vision and Pattern Recognition, pp. 770–778 (2016)